

# PROJECT DESCRIPTION

## Results from Prior NSF Support

**AWARD:** NSF Arctic Natural Sciences Grant ARC-0934721, 10/01/2009 – 09/30/2014; Collaborations in Mathematical Geosciences (CMG): *Mathematics and Electromagnetics for Monitoring Transport Processes in Sea Ice*, PI: K. M. Golden, Co-PI's: Hajo Eicken (U. of Alaska, Fairbanks), Elena Cherkaev, Jingyi Zhu, Cynthia Furse (EE), \$850,000.

**Summary of activities and results:** This project is aimed at developing the mathematical and electromagnetic methods necessary to remotely monitor the internal state of sea ice, its porous brine microstructure, and fluid and thermal transport through the ice. Such developments can help track key transitions in the state of polar sea ice and improve projections of its fate and impact on ecosystems. Toward these goals we have conducted field experiments on the fluid and electromagnetic transport properties of sea ice in the Arctic in 2011, 2012, and 2013, and in the Antarctic in 2010 and 2012. Fluid flow through sea ice mediates a broad range of geophysical and biological processes in the polar marine environment. For example, the evolution of melt ponds and summer ice albedo is constrained by drainage through porous sea ice [31]. Fluid flow also facilitates snow-ice formation [84], the evolution of the salt budget [141], convection-enhanced thermal transport [83], CO<sub>2</sub> exchange [112], and biomass build-up sustained by nutrient fluxes [141, 38]. However, for brine volume fractions below about 5%, columnar sea ice is effectively impermeable to fluid flow, while it is increasingly permeable for volume fractions above 5%. This critical behavior of fluid transport controls the above processes, and is known as the *rule of fives* [50, 54, 108]. In two different experiments conducted in the Arctic and Antarctic, we have found that this critical threshold for fluid flow exhibits a strong, characteristic electrical signature [53]. Sea ice conductivity data are accurately explained by percolation theory, with the same universal critical exponent of 2 which captures the behavior of the fluid permeability [54]. The data also indicate marked changes in the conductivity profile with the onset of melt ponds. In fact, based on rigorous relations between fluid and electrical transport, we are able to partition the range of measured resistivity values into intervals corresponding to distinct regimes of permeability characteristics and related processes, such as melt pond development, and fluxes of nutrients and CO<sub>2</sub>.

We have also constructed a network model of electrical transport in sea ice [147]. It is built on an earlier network model of fluid flow through sea ice [148], to help explain our experimental results and provide further understanding of how fluid and electrical transport are related. We have developed a fundamental, rigorous mathematical method for recovering microstructural information about sea ice from electromagnetic measurements [101]. In particular, we obtained the first results on inverting effective complex permittivity data for information about the connectedness of inclusions in a composite, and applied these results to sea ice. Moreover, we have found a mathematical method for finding rigorous bounds on the complex permittivity of polycrystalline composites, and applied them to sea ice, given information on the statistics of crystal orientations [61]. We obtain inverse bounds as well, which we expect to be pivotal in electromagnetically distinguishing between columnar and granular crystalline microstructures, which have different fluid transport properties [116]. With Daniel Liu (West High School student) and Jingyi Zhu (Associate Professor of Mathematics) we have treated the challenge of finding the thermal conductivity of sea ice as an inverse problem. The “best” composite structures which fit the thermal profile data from a 2007 Antarctic expedition are found. We have computed the effective thermal behavior [81], and also begun to look for enhancement due to brine convection, and we do see strong evidence of this. Please see PI's bio for outreach.

**AWARD:** NSF Division of Mathematical Sciences Grant DMS-0940249, 10/01/2010 – 09/30/2015; Collaborative Research: *Mathematics and Climate Change Research Network*, PI: C. Jones (UNC, Chapel Hill), Co-PI's: K. M. Golden, H. Kaper (Georgetown), M. L. Zeeman (Bowdoin), (\$527,727 to U. of Utah, one of 12 hubs), total funding \$5,000,000.

**Summary of activities and results:** The goal of the math climate research network (MCRN) – the first of its kind funded by the NSF Division of Mathematical Sciences – is to bring to bear mathematics to fundamental problems of climate change, and to help younger mathematicians get involved in this type of research. In our research program at the University of Utah funded by this grant, we have focused on our long term program of treating multiscale sea ice problems with methods from composite materials and statistical physics. This grant has also partially supported the polar expeditions mentioned above. One of

our principal studies has concerned the evolution of the geometrical structure of Arctic melt ponds. During the Arctic melt season, the sea ice surface undergoes a remarkable transformation from vast expanses of snow covered ice to complex mosaics of ice and melt ponds. Sea ice albedo, a key parameter in climate modeling [34, 118, 104, 107], is determined by the complex evolution of melt pond configurations. In fact, ice-albedo feedback has played a major role in the recent declines of the summer Arctic sea ice pack [106]. However, understanding melt pond evolution remains a significant challenge to improving climate projections [34]. By analyzing area–perimeter data from hundreds of thousands of melt ponds, we found an unexpected separation of scales, where pond fractal dimension  $D$  transitions from 1 to 2 around a critical length scale of 100 square meters in area [64]. Pond complexity increases rapidly through the transition as smaller ponds coalesce to form large connected regions, and reaches a maximum for ponds larger than 1000 square meters whose boundaries resemble space filling curves with  $D \approx 2$  [113]. These universal features of Arctic melt pond evolution are similar to phase transitions in statistical physics [25, 142, 26]. The results impact sea ice albedo, the transmitted radiation fields under melting sea ice [37], the heat balance of sea ice and the upper ocean, and biological productivity such as under ice phytoplankton blooms. We have developed a version of the ferromagnetic Ising model [25, 142] to describe melt ponds, and noted striking similarities of regions of like “spins” with melt pond configurations [138]. With Brady Bowen (began with PI as a freshman) we have used continuum percolation models [66], where regions of intersection between a plane and a random surface, representing snow and ice topography, resemble melt ponds [10]. With Rebecca Nickerson (West High School student) we have developed an interacting particle system model, based on the voter model, where a square is more likely to melt if its neighbors have melted [100]. Again, the configurations closely resemble melt ponds, and exhibit the transition in fractal dimension.

With Lorenz Postdoctoral Fellow Ivan Sudakov we have been investigating the implications of the transition in fractal geometry exhibited by melt ponds and its impact on ice-albedo feedback. Sudakov has also been looking at the existence of bifurcations in dynamical system models of Arctic sea ice and permafrost melting and methane release. Another direction we have pursued is to begin to develop mathematical techniques for *upscaling* local information about sea ice to obtain effective properties on larger scales. In the analytic continuation method for studying the effective properties of composites [43, 4, 90] (see below), the microstructural characteristics of a composite are incorporated into integral representations of its effective properties through a *spectral measure* of a self-adjoint operator which depends only on the composite microgeometry. In an initial study of this type, we have computed the spectral measures for human bone, whose microstructure is similar to the porous microstructure of sea ice, to analyze the connectivity of the bone and its relation to osteoporosis [56]. For a discretized image of any composite structure, independent of the length scale, the computation of the spectral measure reduces to finding the eigenvalues and eigenvectors of a symmetric matrix [94]. We have carried out such computations for examples of the brine phase in sea ice, melt ponds on the surface of Arctic sea ice, and the sea ice pack itself [98]. We have also discovered that the eigenvalue spacing distributions of these composites exhibit striking transitions as connectivity thresholds are reached [96]. Such distributions are being investigated in an important area of mathematics – random matrix theory. Our work in random matrices here connects problems in polar climate change to this exciting area of math (and will be pursued further here). Please see PI’s bio for outreach.

**AWARD:** NSF Arctic Natural Sciences Grant ARC-1022485, 8/15/2010 – 8/14/2014, U. of Utah, *Negative sea ice-circulation feedback along Arctic marginal ice zones*. PI: C. Strong, \$242,991.

**Summary of activities and results:** This project in its final year focuses on a negative feedback process involving the winter Arctic marginal ice zone (MIZ) over the Barents Sea. In this feedback process, sea ice concentration anomalies generate heat flux anomalies, which alter surface wind stresses that in turn operate on the sea ice. Decomposing the sea ice-atmosphere feedback using sequential boundary forcing experiments over the Barents Sea, we found that thermodynamic effects provided a dominant positive feedback and dynamic effects provided a weaker negative feedback [80, 77]. To further explore this intriguing result, we developed a module for the NCAR Community Climate System Model which allows us to selectively suppress the sea ice-to-atmosphere component of the feedback, and we have experiments underway using the new framework to investigate the feedback’s impacts on atmospheric and sea ice variability.

In addition to the above-described coupled framework for feedback suppression experiments, new analytical methods emerging from this project include objective measurement of MIZ width [122, 124, 125, 136] and objective identification of propagating atmospheric patterns important to geographically fixed variations

[127] including sea ice flux [75, 76]. As part of the outreach for this project, PI Strong visits minority-populated area high schools to show students how to access and work with climate data and simple climate models. So far, Co-PI Strong and his graduate student acknowledge support from this project in six peer reviewed manuscripts [124, 127, 76, 137, 80, 77], and ten invited seminars or conference proceedings [122, 123, 75, 74, 125, 128, 126, 78, 79, 136].

**AWARD:** NSF Division of Atmospheric Sciences grant ATM-0612779, 2/01/2008 – 06/30/2009, U. of California, Irvine, *Forcings and Feedbacks: Arctic Sea Ice and the Atmosphere*. PI: G. Magnussdottir (U. of California, Irvine), Postdoctoral researcher: C. Strong.

**Summary of activities and results:** PI Strong's NSF-supported postdoctoral work with Gudrun Magnussdottir focused on the interaction between variability in sea ice and the overlying atmospheric circulation, especially with regard to the NAO and feedback processes. Statistically testable definitions of causality and feedback [57] were used to detect a negative feedback between the North Atlantic Oscillation (NAO) and the leading pattern of winter sea ice variability over the North Atlantic in observations [135]. Analyses indicated that this sea ice-NAO interaction will persist over the next three centuries, but change in form under projected declines in sea ice extent [133]. To quantify the effects of feedback in the sea ice-NAO system, Strong customized the NCAR atmospheric global climate model (CAM 3) so that sea ice anomalies on the lower boundary were stochastic with adjustable sensitivity to the model's evolving NAO index ( $N$ ). Using the customized CAM 3 and a vector autoregressive statistical model, Strong [132] showed that the variance of  $N$  depends inversely and approximately linearly on the strength of negative feedback in the system.

Strong [134] presented evidence that tropospheric Rossby wave breaking (RWB) is vital to the dynamics by which NAO-driven sea ice anomalies feed back onto the NAO. This finding was enabled by a method for objective detection and analysis of RWB that Strong developed during the NOAA-supported portion of his postdoctoral work [130, 131]. Combining the RWB detection algorithm with a wave activity flux diagnostic [63] revealed that tropospheric RWB over the Pacific can trigger sign changes in the NAO [129]

## 1 Introduction

Earth's sea ice packs form a key component of Earth's climate system, and are sensitive indicators of climate change. They cover the polar oceans in winter, and recede in summer. During the summers of the 1980's and 1990's, sea ice still covered most of the Arctic basin. However, over just the past decade or so about half of this extensive summer ice pack has melted. While global climate models generally predict sea ice declines over the 21<sup>st</sup> century, these precipitous losses have significantly outpaced most projections [120, 8]. One of the fundamental challenges of climate science is to develop more rigorous representations of sea ice in climate models, and account for important sub-grid scale processes and structures to improve projections. Developing mathematics to analyze effective behavior on larger scales relevant to climate models is at the heart of advancing our understanding of Earth's climate and the role that the sea ice packs play in its evolution.

Sea ice forms the thin boundary layer between the ocean and atmosphere in the polar regions, and is a critical component of the world's ocean system, as well as a leading indicator of climate change [146, 68, 141, 120]. The sea ice packs mediate the exchange of heat, moisture and momentum between the ocean and atmosphere, the two principal geophysical fluids on Earth. For example, as winds push sea ice around on the ocean surface, momentum is transferred to the water below; the rougher the ice, the more efficient the transfer. This process can cause large-scale overturning in the upper ocean, bringing warmer water to the surface. As another example, when sea ice freezes, it rejects cold, dense brine, forming descending plumes in the polar oceans. In the Southern Ocean, this process leads to the formation of Antarctic *bottom water*, which then flows like a complex river through the world's oceans. Likewise, the input of fresher water into the upper ocean during the melt season is also important. Another process in atmosphere–ocean interactions is the transfer of heat between them. In winter when the ocean is warmer, heat flows to the atmosphere through the sea ice itself, which forms an insulating blanket over the ocean, as well as through *leads* or openings in the pack. The thermal conductivity of sea ice is thus an important transport coefficient helping to quantify atmosphere–ocean interactions in coupled climate models, as is sea ice concentration – the area fraction  $\psi$  of the ocean covered by sea ice.

**Sea ice albedo:** One of the principal roles that sea ice plays is in reflecting much of the solar radiation that is incident on Earth’s surface in the polar regions. Roughly speaking, most of the solar radiation incident on snow-covered sea ice is reflected, while most of the sunlight incident on darker sea water or melt water on the surface of the ice is absorbed. Sea ice is both an ocean sunscreen and blanket, preventing solar rays from warming the waters beneath and thwarting ocean heat from escaping to warm the air above. The ratio of reflected sunlight to incident sunlight is called *albedo*. While the albedo of snow-covered ice is close to 1 (larger than 0.8), the albedo of sea water is close to zero (less than 0.1). The overall or effective albedo of the sea ice pack is a significant source of uncertainty in climate projections [7] and a fundamental problem in climate modeling [34, 118, 104, 107].

As warming temperatures melt sea ice over time, fewer bright surfaces are available to reflect sunlight, more heat escapes from the ocean to warm the atmosphere, and the ice melts further. As more ice is melted, the albedo of the polar oceans decreases, leading to more solar absorption and warming, which in turn leads to more melting, in a positive feedback loop. It is believed that this so-called *ice-albedo feedback* has played an important role in the recent dramatic declines in summer Arctic sea ice extent [105, 106]. Thus, even a small increase in temperature can lead to greater warming over time, making the polar regions the most sensitive areas to climate change on Earth. Global warming is *amplified* in the polar regions [119]. Indeed, global climate models consistently show amplified warming in the high latitude Arctic, although the magnitude varies considerably across different models. For example, the average surface air temperature at the North Pole by the end of the 21<sup>st</sup> century is predicted to rise by a factor of about 1.5 to 4 times the predicted increase in global average surface air temperature.

**Multiscale structure of sea ice:** One of the fascinating, yet challenging aspects of modeling sea ice and its role in global climate is the sheer range of relevant length scales of structure, over ten orders of magnitude from the submillimeter scale to hundreds of kilometers. Modeling sea ice on a large scale depends on some understanding of the physical properties of sea ice at the scale of individual floes and even smaller. Today’s climate models challenge the most powerful super computers to their fullest capacity. However, even the largest computers still limit the horizontal resolution to tens of kilometers and require clever approximations and parameterizations to model the basic physics of sea ice. One of the central themes is how to use information on smaller scales to predict behavior on larger scales. We observe here that this central problem of climate science shares commonality with the key challenges, for example, in statistical mechanics and theories of the effective properties of composites.

**Transport in sea ice:** Let’s focus briefly on sea ice microphysics – fluid and electromagnetic transport in sea ice, where we have done extensive theoretical work as well as field measurements on the effective or homogenized properties of the ice [49, 42, 50, 52, 51, 55, 54, 48, 101, 148, 147, 53]. This work provides a *road map* as to the types of ideas and mathematical methods which can treat rigorously the effective properties of multiscale composites such as sea ice on larger scales.

Sea ice is a porous composite of pure ice with liquid brine inclusions. These inclusions host extensive algal and bacterial communities which support life in the polar oceans [141, 38]. The flow of fluids through sea ice mediates processes important to climate such as melt pond drainage, which is critical to the evolution of sea ice albedo. Fluid flow through sea ice also governs the evolution of the salt budget and salinity profiles [141], convection-enhanced thermal transport [83], ocean-ice-atmosphere CO<sub>2</sub> exchanges [111], and the build-up of algal biomass fueled by fluxes of nutrients [141, 38]. It also drives snow-ice formation, which accounts for a significant portion of the ice produced in the Southern Ocean [84]. Sea water percolates upward through the porous brine microstructure, flooding the snow layer, which subsequently freezes.

Sea ice exhibits a very interesting and important critical phenomenon [50]. For brine volume fractions  $\phi$  below about 5%, columnar sea ice is effectively impermeable to fluid flow, while for  $\phi$  above 5%, it is increasingly permeable. The critical brine volume fraction  $\phi_c \approx 5\%$  corresponds to a critical temperature  $T_c \approx -5^\circ$  for a typical bulk sea ice salinity of 5 parts per thousand. This critical behavior in the fluid flow properties of sea ice, occurring at this particular threshold, is known as the *rule of fives*. Given the broad range of processes which are governed by fluid flow through the porous microstructure of the ice, this rule can be thought of, roughly speaking, as the *on-off switch* for fluid flow in sea ice. Understanding how the fluid permeability of sea ice depends on temperature  $T$  or brine volume fraction  $\phi$  is prerequisite to incorporating processes governed by fluid flow into climate models.

In a series of papers we employed mathematical methods of composite materials and statistical physics [48] to develop rigorous bounds [55], and percolation [50, 54, 108, 116], network [148] and hierarchical

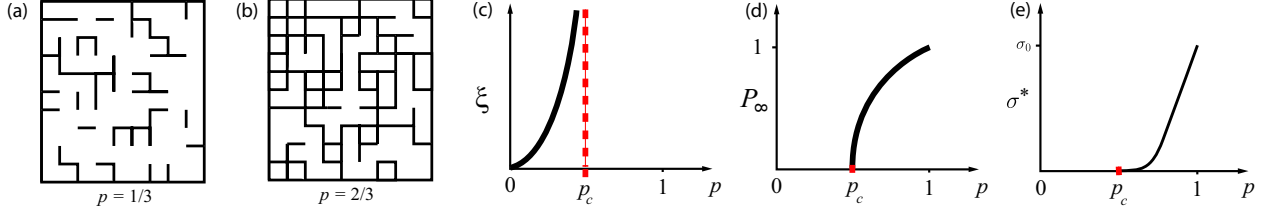


Figure 1: The two dimensional square lattice percolation model below its percolation threshold of  $p_c = 1/2$  in (a) and above it in (b). (c) Divergence of the correlation length as  $p$  approaches  $p_c$ . The infinite cluster density of the percolation model is shown in (d), and the effective conductivity is shown in (e).

models [54] for fluid transport in sea ice. In particular, we obtained simple formulas for the vertical fluid permeability of sea ice as a function of  $\phi$ , which are being used in work incorporating melt pond evolution into climate models [34, 35]. Moreover, X-ray computed tomography and mapping of the pore microstructure onto random graphs was used to demonstrate that the brine phase of sea ice undergoes a transition in connectedness, or *percolation threshold*, at the critical brine volume fraction [54, 108]. Percolation theory was used to theoretically predict the transition, and to mathematically characterize the thermal evolution of the fluid pores and their connectedness [50, 54, 108]. Lattice and continuum percolation models of transport are used to predict critical behavior of the fluid permeability and electrical conductivity in sea ice, with a universal exponent describing the behavior above the percolation threshold [54, 53, 116].

We have also made extensive use of methods of homogenization, and the analytic continuation method in particular, to study the electromagnetic properties of sea ice such as its effective complex permittivity over a range of frequencies [49, 42, 52, 46, 48]. Moreover, we have developed methods of *inverse homogenization* to recover microstructural properties and information about the spectral measure from measurements of effective properties on larger scales [24, 51, 60, 56, 101]. Here we propose to address similar issues of microstructure and macroscopic, effective behavior, but for composite structure of sea ice on length scales more relevant to climate modeling.

## 2 Mathematical models of composites and phase transitions

Here we give a brief overview of some of the mathematical models and techniques that we will use in studying the effective properties of the sea ice pack.

**Percolation models.** Consider the  $d$ -dimensional integer lattice  $\mathbb{Z}^d$ , and the square or cubic network of bonds joining nearest neighbor lattice sites. In the percolation model [12, 121, 58, 16], we assign to each bond a conductivity  $\sigma_0 > 0$  with probability  $p$ , meaning it is open (black), and with probability  $1 - p$  we assign a 0, meaning it is closed. Two examples of lattice configurations are shown in Figure 1, with  $p = 1/3$  in (a) and  $p = 2/3$  in (b). Groups of connected open bonds are called *open clusters*. In this model there is a critical probability  $p_c$ ,  $0 < p_c < 1$ , called the *percolation threshold*, at which the average cluster size diverges and an infinite cluster appears. For the two dimensional bond lattice  $p_c = 1/2$ . For  $p < p_c$  the density of the infinite cluster  $P_\infty(p)$  is 0, while for  $p > p_c$ ,  $P_\infty(p) > 0$  and near the threshold,  $P_\infty(p) \sim (p - p_c)^\beta$  as  $p \rightarrow p_c^+$ , where  $\beta$  is a universal critical exponent, that is, it depends only on dimension and not on the details of the lattice. Let  $x, y \in \mathbb{Z}^d$  and  $\tau(x, y)$  be the probability that  $x$  and  $y$  belong to the same open cluster. Then for  $p < p_c$ ,  $\tau(x, y) \sim e^{-|x-y|/\xi(p)}$ , and the correlation length  $\xi(p) \sim (p_c - p)^{-\nu}$  diverges with a universal critical exponent  $\nu$  as  $p \rightarrow p_c^-$ , as shown in Figure 1 (c).

The effective conductivity  $\sigma^*(p)$  of the lattice, now viewed as a random resistor (or conductor) network, defined via Kirchoff's laws, vanishes for  $p < p_c$  like  $P_\infty(p)$  since there are no infinite pathways, as shown in Figure 1 (e). For  $p > p_c$ ,  $\sigma^*(p) > 0$ , and near  $p_c$ ,  $\sigma^*(p) \sim \sigma_0(p - p_c)^t$ ,  $p \rightarrow p_c^+$ , where  $t$  is the conductivity critical exponent, with  $1 \leq t \leq 2$  in  $d = 2, 3$  [40, 41, 47], and numerical values  $t \approx 1.3$  in  $d = 2$  and  $t \approx 2.0$  in  $d = 3$  [121]. Consider a random pipe network with effective fluid permeability  $k^*(p)$  exhibiting similar behavior  $k^*(p) \sim k_0(p - p_c)^e$ , where  $e$  is the permeability critical exponent, with  $e = t$  [18, 115, 47]. Both  $t$  and  $e$  are believed to be universal – they depend only on dimension and not the lattice. Continuum models can

exhibit nonuniversal behavior with exponents different from the lattice case and  $e \neq t$  [62, 33, 121, 114, 73].

**Analytic continuation and spectral measures.** *Homogenization* denotes a field of applied mathematics where the goal is to find a homogeneous medium which behaves macroscopically the same as a given inhomogeneous medium. The methods are focused on finding the effective properties of inhomogeneous media such as composites. We will see that the *spectral measure* provides a powerful tool for upscaling geometrical information about a composite into calculations of effective properties.

We now briefly describe the *analytic continuation method* (ACM) for studying the effective transport properties of composite materials [5, 90, 43, 46]. Later we will show how this method may be adapted to studies of polycrystalline media [94, 3] and advection enhanced diffusion of passive tracers by incompressible fluid velocity fields [1, 2]. This method has been used to obtain rigorous bounds on effective transport coefficients of two-component [5, 90, 43, 6, 13] and multicomponent [39, 44] composite materials, as well as uniaxial polycrystalline media [61, 94] and complex fluid flows [1, 2]. These bounds follow from the special analytic structure of the representations for the effective parameters, and partial knowledge of the microstructure, such as the relative volume fractions of the phases in the case of composite media.

For simplicity, we consider the electrical conductivity tensor  $\sigma$  of a two-phase random medium, although the method applies to any classical transport coefficient [92]. Here,  $\sigma(x, \omega)$  is a (spatially) stationary random field in  $x \in \mathbb{R}^d$  and  $\omega \in \Omega$ , where  $\Omega$  is the set of all geometric realizations of the medium, which is indexed by the parameter  $\omega$  representing one particular realization, and the underlying probability measure  $P$  is compatible with stationarity [43]. The propagation properties of an electromagnetic wave in a given composite medium is determined by the quasi-static limit of Maxwell's equations [67, 43]

$$\nabla \times E = 0, \quad \nabla \cdot J = 0, \quad J = \sigma E, \quad \langle E \rangle = e_k, \quad (1)$$

where  $E(x, \omega)$  and  $J(x, \omega)$  are stationary electric and current fields, respectively,  $e_k$  is a standard basis vector in the  $k^{\text{th}}$  direction, and  $\langle \cdot \rangle$  denotes ensemble averaging over  $\Omega$  or spatial average over all of  $\mathbb{R}^d$  [43]. The effective complex conductivity tensor  $\sigma^*$  is defined by [43]

$$\langle J \rangle = \sigma^* \langle E \rangle. \quad (2)$$

The linear constitutive relation  $J = \sigma E$  in (1) relates the local intensity and flux, while the linear relation in (2) relates the mean intensity and mean flux.

Since we are dealing with a two-phase locally isotropic medium, the components  $\sigma_{jk}$  of  $\sigma$  satisfy  $\sigma_{jk}(x, \omega) = \sigma(x, \omega)\delta_{jk}$ , where  $\delta_{jk}$  is the Kronecker delta and

$$\sigma(x, \omega) = \sigma_1 \chi_1(x, \omega) + \sigma_2 \chi_2(x, \omega). \quad (3)$$

Here,  $\sigma_j$  is the *complex* value of the conductivity for medium  $j = 1, 2$  and  $\chi_j(x, \omega)$  is its characteristic function, equaling 1 for  $\omega \in \Omega$  with medium  $j$  at  $x$ , and 0 otherwise, with  $\chi_2 = 1 - \chi_1$ . For simplicity, we focus on one diagonal coefficient  $\sigma^* = \sigma_{kk}^*$ , with  $\sigma^* = \langle \sigma E \cdot e_k \rangle$ . By the homogeneity of  $\sigma(x, \omega)$  in (3),  $\sigma^*$  depends on the contrast parameter  $h = \sigma_1/\sigma_2$  and we define  $m(h) = \sigma^*/\sigma_2$ , which is a Herglotz function that maps the upper half  $h$ -plane to the upper half plane, and is analytic off  $(-\infty, 0]$  [4, 43].

The key step in the method [43, 4, 90, 92] is obtaining a Stieltjes integral representation for  $\sigma^*$ . This integral representation arises from a resolvent representation of the electric field [43, 95]  $E = s(sI - \Gamma\chi_1)^{-1}e_k$ , where  $\Gamma = \nabla(\Delta^{-1})\nabla \cdot$  acts as a projection from  $L^2(\Omega, P)$  onto the Hilbert space of curl-free random fields [43], and  $\Delta^{-1}$  is based on of convolution with the free space Green's function for the Laplacian  $\Delta = \nabla^2$ . Consider the function  $F(s) = 1 - m(h)$ ,  $s = 1/(1 - h)$ , which is analytic off  $[0, 1]$  in the  $s$ -plane. Then writing  $\sigma = \sigma_2(1 - \chi_1/s)$  in (3) yields [43, 109]

$$F(s) = \langle \chi_1[(sI - \Gamma\chi_1)^{-1}e_k] \cdot e_k \rangle = \int_0^1 \frac{d\mu(\lambda)}{s - \lambda}, \quad s = \frac{1}{1 - \sigma_1/\sigma_2}, \quad (4)$$

where  $\mu(d\lambda) = \langle \chi_1 Q(d\lambda) e_k \cdot e_k \rangle$  is a positive *spectral measure* on  $[0, 1]$  and  $Q(d\lambda)$  is the (unique) projection valued measure associated with the random, bounded, self-adjoint operator  $\Gamma\chi_1$  [43, 95].

Equation (4) is based on the spectral theorem [109] for the resolvent of the operator  $\Gamma\chi_1$ . It provides a Stieltjes integral representation for the effective complex conductivity  $\sigma^*$  which separates the component parameters in  $s$  from the complicated geometrical information contained in the measure  $\mu$ . (Extensions of (3) to multicomponent media with  $\sigma = \sigma_1\chi_1 + \sigma_2\chi_2 + \sigma_3\chi_3 + \dots + \sigma_n\chi_n$  involve several complex variables [44, 39, 93, 91, 30]). Information about the geometry enters through the moments  $\mu_n = \int_0^1 \lambda^n d\mu(\lambda) = \langle \chi_1[(\Gamma\chi_1)^n e_k] \cdot e_k \rangle$ ,  $n = 1, 2, 3, \dots$ . For example, the mass  $\mu_0$  is given by  $\mu_0 = \langle \chi_1 e_k \cdot e_k \rangle = \langle \chi_1 \rangle = \phi$ , where

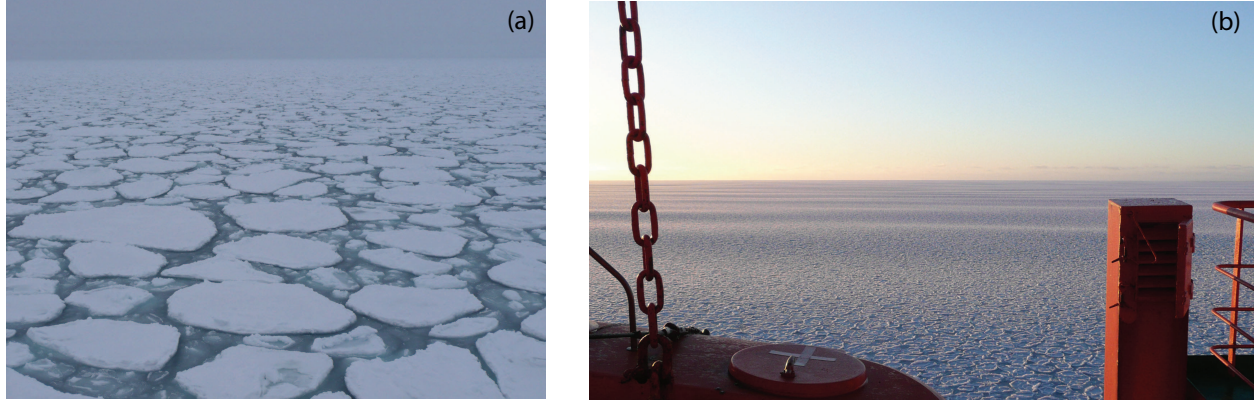


Figure 2: (a) Sea ice broken into floes in the marginal ice zone off of Wilkes Land, Antarctica, photographed by Co-PI Golden during the 2007 Sea Ice Physics and Ecosystem eXperiment (SIPEX). The larger floes in the foreground are 2 to 3 meters across, and are separated by frazil ice. (b) A vast field of pancake ice interacting with ocean swells in the marginal ice zone off the coast of East Antarctica, photographed by Golden during SIPEX. The larger floes in the foreground are approximately 1 meter across.

$\phi$  is the volume or area fraction of material phase 1, such as the open ocean coverage, and  $\mu_1 = \phi(1 - \phi)/d$  if the material is statistically isotropic [43, 14]. In general,  $\mu_n$  depends on the  $(n + 1)$ -point correlation function of the medium.

Computing the spectral measure  $\mu$  for a given composite microstructure first involves discretizing a two phase image of the composite into a square lattice filled with 1's and 0's corresponding to the two phases. Then the key operator  $\Gamma_{\chi_1}$ , which depends on the geometry via  $\chi_1$ , becomes a self adjoint matrix. The spectral measure may be calculated directly from the eigenvalues and eigenvectors of this matrix.

### 3 Proposed research

#### 3.1 Geometry of the marginal ice zone

Dense pack ice transitions to open ocean over a region of broken ice termed the marginal ice zone (MIZ; Fig. 2) – a highly dynamic region where the ice cover lies close to an open ocean boundary and intense atmosphere–ice–ocean interactions take place [e.g., 82]. The width of the MIZ is a fundamental length scale for polar dynamics [e.g., 145] in part because it represents the distance over which ocean waves and swell penetrate into the sea ice cover. Wave penetration can break a smooth ice layer into floes, as shown in Fig. 2a, meaning the MIZ acts as a buffer zone that protects the stable morphology of the inner ice. Waves also promote the formation of pancake ice, as shown in Fig. 2b. Moreover, the width of the MIZ is an important spatial dimension of the marine polar habitat and impacts human accessibility to high latitudes. In [137] a dramatic 39% widening of the summer Arctic MIZ based on objective analysis of three decades of satellite–derived sea ice concentrations (1979–2012) was reported.

Challenges associated with objective measurement of the MIZ width include the MIZ shape, which is in general not geodesically convex, as illustrated by the example shaded white in Fig. 3a. Sea ice concentration ( $c$ ) is used here to define the MIZ as a body of marginal ice ( $0.15 \leq c \leq 0.80$ ) adjoining both pack ice ( $c > 0.80$ ) and sparse ice ( $c < 0.15$ ). To define an objective MIZ width applicable to such shapes, Strong [124] introduced the idea of an idealized sea ice concentration field  $\psi(x, y)$  satisfying Laplace's equation within the MIZ,

$$\nabla^2 \psi = 0. \quad (5)$$

We use  $(x, y)$  to denote a point in two dimensional space, and it is understood that we are working on the spherical Earth. The solution to (5) for the example in Fig. 3a is shown by color shading in Fig. 3b. Any curve  $\gamma$  orthogonal to the level curves of  $\psi$  and connecting two points on the MIZ perimeter (a field line through the gradient field  $\nabla \psi$ ; black curves, Fig. 3b) is contained in the MIZ, and its length provides an objective



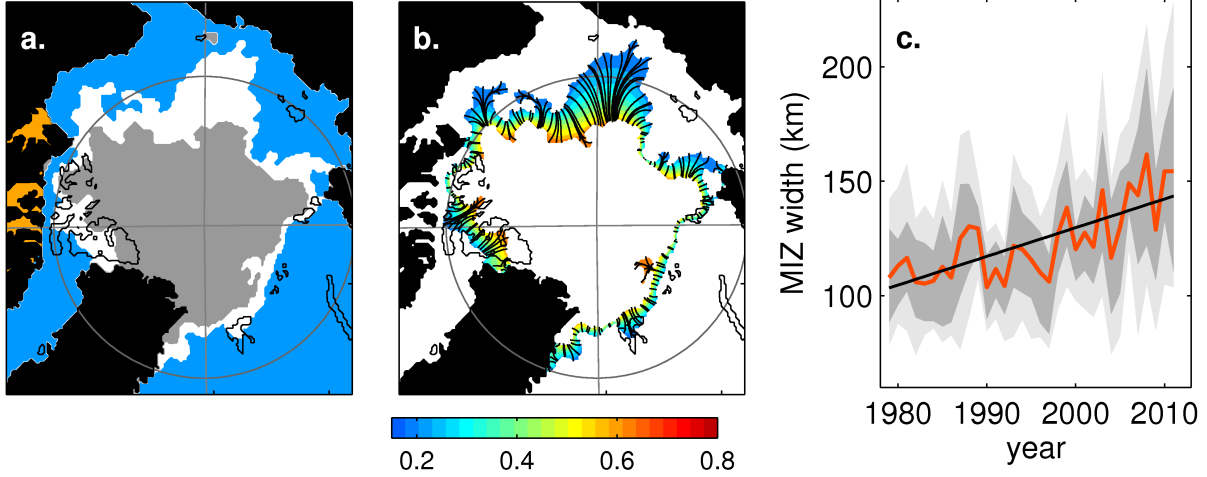


Figure 3: (a) Based on satellite derived sea ice concentrations on 29 August 2010: pack ice (gray;  $c > 0.80$ ), marginal ice zone (white;  $0.15 \leq c \leq 0.80$ ), and sparse ice (blue;  $c < 0.15$ ). Orange shading shows semi-enclosed water bodies and black curves show small islands over which sea ice concentrations were interpolated. (b) Shading shows solution to Laplace's equation within the MIZ ( $\psi$ ), and width measurements following the gradient of  $\psi$  are black curves (only subset shown for clarity). (c) Width of the summer (July-September) marginal ice zone for 1979-2011 (red curve). Percentiles of daily MIZ widths are shaded dark gray (25<sup>th</sup> to 75<sup>th</sup>) and light gray (10<sup>th</sup> to 90<sup>th</sup>). Results are adapted from [137] and are based on analysis of data from the National Snow and Ice Data Center [89].

measure of MIZ width ( $\ell$ ). Defined in this way,  $\ell$  is a function of distance along the MIZ perimeter ( $s$ ) from an arbitrary starting point, and this dependence is denoted  $\ell = \ell(s)$ . Analogous applications of Laplace's equation have been introduced in medical imaging to measure the width or thickness of human organs, and [70] details some desirable mathematical properties of the technique including rotational invariance.

Boundary conditions for (5) are  $\psi = 0.15$  where MIZ borders a sparse ice region and  $\psi = 0.80$  where the MIZ borders a pack ice region. Derivatives in (5) were numerically approximated using second-order finite differences, and solutions were obtained in the data's native stereographic projection since solutions of Laplace's equation are invariant under conformal mapping [e.g., 117]. For a given day and MIZ, a summary measure of MIZ width ( $w$ ) can be defined by averaging  $\ell$  with respect to distance along the MIZ perimeter

$$w = \frac{1}{L_M} \int_M \ell(s) ds \quad (6)$$

where  $M$  is the closed curve defining the MIZ perimeter and  $L_M$  is the length of  $M$ . Averaging  $w$  over July-September of each available year reveals the dramatic widening of the summer MIZ (Fig. 3c).

**Extended analysis:** Here, we propose a more general form of (5),

$$\nabla \cdot (\sigma \nabla \psi) = 0 \quad (7)$$

which is a natural generalization, both mathematically and physically, of (5). The introduction of a local conductivity field  $\sigma = \sigma(x, y)$  or a local diffusivity field  $D = D(x, y)$  will enable the idealized sea ice concentration field  $\psi$  to more faithfully reflect sea ice rheology and variability, with fluctuations in  $\psi(x, y)$  related to the inhomogeneities in  $\sigma$  or  $D$ . In particular, in the electrical analogue,  $\vec{E} = -\nabla \psi$  plays the role of an electric field, with  $\vec{J} = \sigma \vec{E}$  an electric current density, as in classical electrodynamics, where  $\psi$  is thought of as an electric potential. Also, we may identify  $J = -D \nabla \psi$  with a diffusive flux density, where  $\nabla \psi$  is a concentration gradient. Then (7) can be written as

$$\nabla \cdot \vec{J} = 0 \quad (8)$$



It is useful to note that (5) can also be interpreted in terms of planar steady state fluid flow. In this context,  $\vec{v} = (u, v) = \nabla\psi$  where  $\psi(x, y)$  is the velocity potential and  $\nabla \cdot \vec{v} = 0$ , which is equivalent to Laplace's equation for  $\psi(x, y)$ .

Consider an actual satellite-derived concentration field  $\psi(x, y)$  satisfying (7) with the boundary conditions above. There is a large body of literature on the so-called *inverse problem* of reconstructing  $\sigma(x, y)$  from information on the potential field  $\psi(x, y)$  on the boundary of the domain, or from measurements of the effective properties of the medium, such as the effective conductivity  $\sigma^*$  associated with  $\sigma(x, y)$  [86, 139, 87, 140, 19, 24, 20, 27, 56, 101, 11]. Here however, the measurements of the potential function  $\psi(x, y)$  are available not only on the boundary of the domain but in the domain as well, which considerably simplifies the recovery problem. However, since the available data are very noisy, we expect that only several lower spherical harmonics in the approximation of  $\sigma(x, y)$  can be reliably reconstructed from such data. The project will develop regularized reconstruction algorithms for reliable recovery of the function  $\sigma(x, y)$ . The numerical stability of such reconstructions will be analyzed. Recovery of lower harmonics of  $\sigma(x, y)$  from spatial variations in  $\psi(x, y)$ , and comparison with oceanic, atmospheric, and thermodynamic forcing will give valuable insights into the components of sea ice physics which are acting to influence  $\psi(x, y)$  and the PDE's modeling its evolution. Because of its more general form, the idealized sea ice concentration field given by (7) will more closely correspond to the observed sea ice field than did the solution from (5).

Finally, we briefly address the development of a time dependent PDE model for the concentration  $\psi(x, y, t)$ . The equation  $\nabla \cdot (D \nabla \psi) = 0$  can be viewed as a steady state heat equation. Thus one natural way of introducing time dependence is through  $\partial\psi/\partial t = \nabla \cdot (D \nabla \psi)$ . However, this equation is limited in that it does not allow for advection of the concentration field through atmospheric, oceanic and thermodynamic forcing. As a first step in this direction, consider a vector field  $\vec{v}$  which captures these forces,

$$\frac{\partial\psi}{\partial t} = \nabla \cdot (D \nabla \psi) - \nabla \cdot (\psi \vec{v}). \quad (9)$$

We will investigate model problems in simplified domains to better understand the role of sea ice physics in MIZ evolution, for model PDE's like the advection diffusion equation in (9). Interestingly, the famous ice thickness distribution equation [110, 65] for  $G(x, y, h, t)$ , the probability density for ice of thickness  $h$  at time  $t$  and position  $(x, y)$ , shares similarities to (9). The concentration function  $\psi(x, y, t)$  is closely related to  $G(x, y, h, t)$  via

$$\psi(x, y, t) = \int_0^\infty G(x, y, h, t) dh. \quad (10)$$

Then the thickness distribution equation is

$$\frac{\partial G}{\partial t} = \Gamma - \nabla \cdot (G \vec{u}) - \frac{\partial}{\partial h}(fG) + \mathcal{L}, \quad (11)$$

where  $\Gamma$  is the mechanical redistribution term (from ridging and leads; not to be confused with the operator  $\Gamma$  in the analytic continuation method),  $\vec{u}$  is the ice velocity field,  $f$  is the rate of freezing, and  $\mathcal{L}$  represents lateral melting and freezing. Integrating (11) in  $h$  from 0 to  $\infty$  yields an equation with similarities to (9). We will explore such connections in developing a sea ice physics based evolution model for  $\psi$ .

A key question is how the reconstructed diffusivity  $D$  (or  $\sigma$ ) is related to the microstructure of the pack or a velocity field as above. If we interpret the larger scale diffusivity field reconstructed from  $\Psi$  as an effective diffusivity, then it could be related via homogenization for the advection diffusion equation (see next section) to smaller scale floe and velocity field structure.

### 3.2 Analytic continuation and spectral measures

Describing the transport properties of complex systems is an important problem which arises throughout the biological and physical sciences, and has a wide variety of engineering and technological applications. Over the years, a broad range of mathematical techniques have been developed that reduce the analysis of complex systems, with rapidly varying structures in space and time, to solving averaged, or *homogenized* equations involving an effective parameter. The goal is to find a homogeneous medium which behaves macroscopically the same as a given inhomogeneous medium, such as a composite material or a fluid velocity field. The methods are focused on finding the effective transport coefficients of a complex system

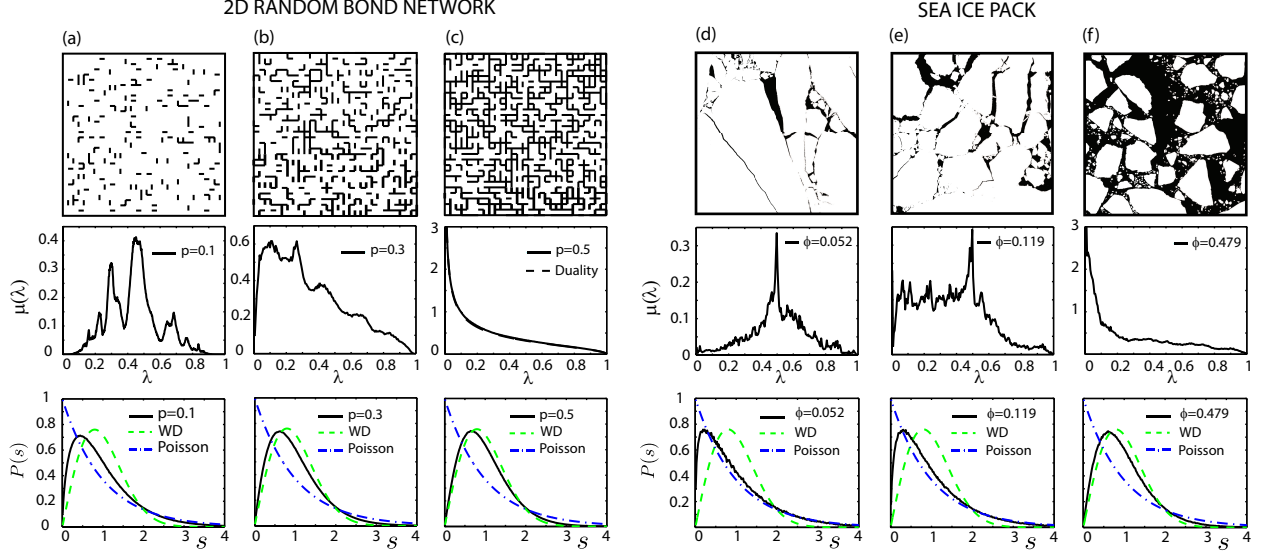


Figure 4: *Spectral upscaling for sea ice structures.* Increasingly connected configurations of the percolation model (a)–(c), and leads in the ice pack (d)–(f), with corresponding spectral functions  $\mu(\lambda)$  and eigenvalue spacing distributions (ESD)  $P(s)$  below. The area under the graph of each spectral function in (d)–(f) is the open water fraction  $\phi = 1 - \psi$ . The eigenvalues in the ESD have been rescaled by an unfolding procedure to have unit mean spacing. For the network, the width of the gaps in the spectrum near  $\lambda = 0, 1$  for  $p = 0.1$  shrink to 0 as the percolation threshold  $p = p_c = 0.5$  is approached, with a subsequent build up of spectra at  $\lambda = 0$  as  $p$  surpasses  $p_c$ . The spectral functions for the ice pack exhibit a similar behavior.

which describe its macroscopic behavior. This discussion provides a framework for the effective transport properties of sea ice, as a polycrystalline material on the cm scale, and a two-phase composite of ice and ocean on the km scale, as well as the effective horizontal diffusive transport of ice floes by advection. We will see that *spectral measures* provide a powerful tool for upscaling local geometric information about these complex systems into calculations of their effective parameters.

A great deal of information can be gleaned from the behavior of the spectral measure itself, through discretizations (finite bond lattice representations) of the continuum [94]. In this case, the action of the operator  $\Gamma\chi_1$  is given by that of a real-symmetric random matrix  $M_1 = \chi_1\Gamma\chi_1$ , where  $\Gamma$  is a (non-random) projection matrix which depends only on the lattice topology and boundary conditions, and  $\chi_1$  is a diagonal (random) projection matrix which determines the geometry and component connectivity of the composite medium. In this case, the spectral measure  $\mu$  is given explicitly in terms of the eigenvalues  $\lambda_i$  and orthonormal eigenvectors  $u_i$  of the matrix  $M_1$  [94]

$$\mu(d\lambda) = \langle Q(d\lambda)\hat{e}_k \cdot \hat{e}_k \rangle, \quad Q(d\lambda) = \sum_i \delta_{\lambda_i}(d\lambda)\chi_1 Q_i. \quad (12)$$

Here,  $\hat{e}_k$  plays the role of a standard basis vector on the lattice,  $Q(d\lambda)$  is the (unique) projection valued measure associated with  $M_1$ ,  $\delta_{\lambda_i}(d\lambda)$  is the delta measure concentrated at  $\lambda_i$ , and  $Q_i = u_i u_i^T$  is the projection matrix associated with the eigenspace spanned by  $u_i$  [94].

From the explicit representation of the spectral measure  $\mu$  displayed in (12), it has been demonstrated that local geometrical information is encoded by “geometric” resonances in  $\mu$  [69], while global connectivity information is encoded by spectral gaps in the support of  $\mu$  located at the spectral endpoints  $\lambda = 0, 1$  [69, 95, 45]. The presence or absence of gaps in the spectrum near  $\lambda = 0, 1$  and the details of how large a gap is or how large the spectral values  $[\chi_1 Q_i \hat{e}_k] \cdot \hat{e}_k$  are, give important information pertaining to the connectivity and effective transport properties of the system. In percolation models, it has been demonstrated that, as the volume fraction of a particular material component increases and the connectivity of the system develops long range order, the gaps shrink and then collapse [69, 95], resulting in the formation of delta components in the measures at  $\lambda = 0, 1$ , *precisely* at the percolation threshold  $p_c$  and  $1 - p_c$  [95]. This leads to critical behavior in the effective transport coefficients of the composite medium.

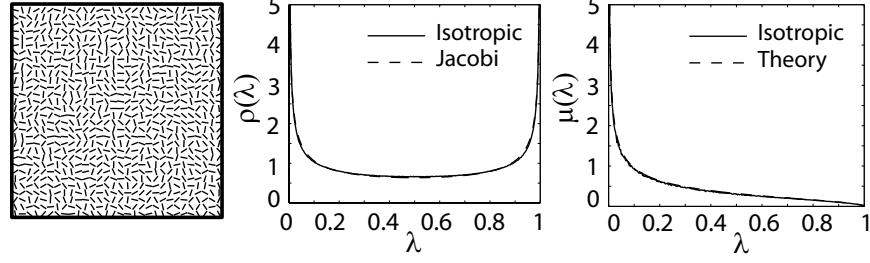


Figure 5: *Spectral analysis of polycrystalline media.* A graphical, lattice representation of a polycrystalline medium which is isotropic within the horizontal plane, with the corresponding eigenvalue density  $\rho(\lambda)$  and spectral function  $\mu(\lambda)$  to the right. The computed eigenvalue density  $\rho(\lambda)$  is displayed with the limiting eigenvalue density for a Jacobi random matrix ensemble  $\rho_J(\lambda) = 1/(\pi\sqrt{\lambda(1-\lambda)})$ . The spectral function  $\mu(\lambda)$  is displayed with its isotropic theoretical prediction [92]  $\mu_I(\lambda) = (\sqrt{(1-\lambda)/\lambda})/\pi$ .

Transitions in the connectedness or percolation properties of a particular material component are also reflected in the behavior of the long and short range eigenvalue correlations of the random matrix  $M_1$  [96]. These statistics indicate that eigenvalues associated with a disordered state, such as a low volume fraction RRN are weakly correlated and well-described by Poisson-like statistics [17, 99]. However, as the percolation transition [121, 144] is approached and the system develops long range order, the eigenvalues become increasingly correlated and their statistics approach classical Wigner-Dyson statistics [59, 28], as in Fig. 4. We see this transition in the spectral gaps and eigenvalue correlations in a variety of composite systems, such as the brine microstructure of sea ice [50, 54] and melt ponds on Arctic sea ice [64].

We propose to explore the large scale effective transport properties of the ice pack and configurations of ice floes, through the lens of random matrix theory and the evolution of eigenvalue statistics and spectral measures. This approach will yield fundamental new insights into the relationship between geometric resonances in the measures and floe geometry, as well as transitions in eigenvalue correlations and spectral gaps in the measures and the percolation properties of floe configurations. This work will help to provide a rigorous way of upscaling microstructural information to progressively larger scales which are relevant to climate models. Moreover, we will utilize our computations of spectral measures in *cross-property* investigations of the effective electromagnetic, thermal and other transport properties, which are *all* completely determined by these measures through the spectral coupling of the governing equations [20, 92, 21, 23].

Our recent analysis [94] of the electromagnetic transport properties of random, uniaxial polycrystalline media has demonstrated that the underlying, rigorous mathematical framework is a direct analogue of that for two-phase random media. For simplicity, we discuss the theory in terms of conductive polycrystalline materials, which are composed of many crystallites (single crystals of varying size, shape, and orientation) that can have different local conductivities along different crystal axes. In the case of uniaxial polycrystalline media, the local conductivity along one of the crystal axes has the *complex* value  $\sigma_1$ , while the conductivity along all the other crystal axes have the value  $\sigma_2$ . The local conductivity tensor of such media is given by [92, 3]  $\sigma(x, \omega) = R^T(x, \omega) \text{diag}(\sigma_1, \sigma_2, \dots, \sigma_2) R(x, \omega)$ , where  $R$  is a rotation matrix, and  $\sigma$  can be written in a form which is a direct analogue of (3), involving the matrix  $C = \text{diag}(1, 0, \dots, 0)$ ,

$$\sigma(x, \omega) = \sigma_1 X_1(x, \omega) + \sigma_2 X_2(x, \omega), \quad (13)$$

where  $X_1 = R^T C R$  is a symmetric projection matrix,  $X_2 = I - X_1$ , and  $X_j X_k = X_j \delta_{jk}$ ,  $j, k = 1, 2$ .

The propagation properties of an electromagnetic wave in a given polycrystalline medium is still determined by (1) (or analog  $D = \epsilon E$  for permittivity), and the effective complex conductivity tensor  $\sigma^*$  is defined by (2). By the symmetries between equations (3) and (13), the method provides a Stieltjes integral representation for the diagonal component  $\sigma^* = \sigma_{kk}^*$  of  $\sigma^*$ , given by equation (4) with  $F(s) = \langle X_1 [(sI - \Gamma X_1)^{-1} e_k] \cdot e_k \rangle$ , involving a positive *spectral measure*  $\mu(d\lambda) = \langle X_1 Q(d\lambda) e_k \cdot e_k \rangle$  on  $[0, 1]$ , where  $Q(d\lambda)$  is the (unique) projection valued measure associated with the random, bounded, self-adjoint operator  $\Gamma X_1$  on  $L^2(\Omega, P)$  with moments  $\mu_n = \langle X_1 [(\Gamma X_1)^n e_k] \cdot e_k \rangle$ . The mass  $\mu_0 = \langle X_1 e_k \cdot e_k \rangle$  of  $\mu$  can be thought of as the percentage of the crystals oriented in the  $k^{\text{th}}$  direction  $e_k$  [3, 94]. Moreover, discretizations of the continuum also lead to the explicit representation of the spectral measure displayed in (12). This enables the direct computation of

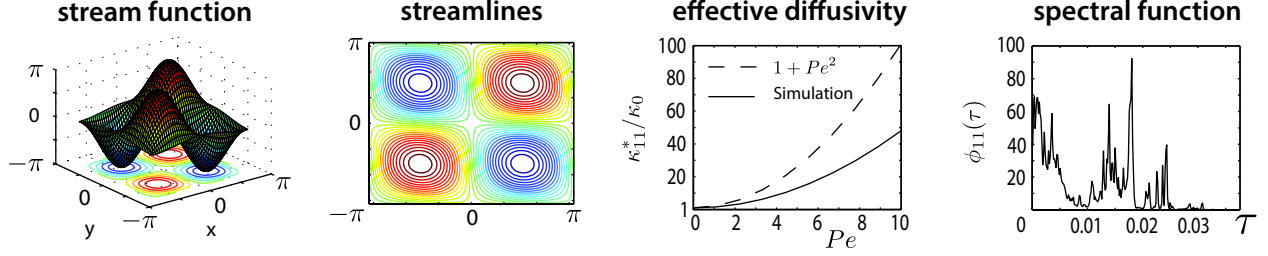


Figure 6: The effective diffusivity and spectral function (histogram representations of the spectral measure) for modified cat's eye flow. The diagonal component  $\kappa_{11}^*$  of the effective diffusivity tensor and spectral function  $\phi_{11}$  are displayed to the right of the corresponding stream function and streamlines. The stream function is given by  $H(x, y) = \sin x \sin y + \eta \cos x \cos y$  with  $\eta$  uniformly distributed in the interval  $(-0.1, 0.1)$ . The theoretical prediction of the effective diffusivity for shear flow in the  $e_1$  direction is  $\kappa_{11}^*/\kappa_0 = 1 + Pe^2$ , which provides a rigorous upper bound.

spectral measures, effective conductivities, and eigenvalue statistics for various orientation statistics.

Via (12), we propose to directly compute spectral measures and effective conductivities corresponding to various crystallite orientation statistics, and investigate the associated electromagnetic transport properties of sea ice as a polycrystalline medium. We will also explore the possible characterization of crystallite microstructure by geometric resonances in the measures, and transitions in the transport properties by behavior of spectral gaps and eigenvalue correlations. An extension of the spectral coupling present in two-component composites to polycrystalline media is also of key interest, so as to recover from the computed spectral measures, the electromagnetic and thermal transport properties of polycrystalline sea ice. The random matrix theory description of sea ice as a polycrystalline medium is a key part of our proposed work. A preliminary computation of the eigenvalue density  $\rho(\lambda)$  corresponding to a two-dimensional polycrystalline medium with *statistically isotropic* crystallite orientation statistics is in striking agreement with the limiting eigenvalue density of a Jacobi random matrix ensemble, as shown in Fig. 5. This provides compelling evidence that the underlying random matrix is a member of this classical ensemble of random matrix theory, which would open this problem up to a broad range of established mathematical techniques [36, 28, 88].

We also propose to generalize this mathematical framework to the case of multi-axial polycrystalline media, with local conductivity tensor given by  $\sigma = R^T \text{diag}(\sigma_1, \sigma_2, \sigma_3, \dots, \sigma_n) R$ . Many of the symmetries between the mathematical frameworks underlying two-component media and that of uniaxial polycrystalline media extend to the multicomponent case. Therefore the existence of such an extension from the well established [44, 39] theory of composite media to multiaxial polycrystalline media is very likely. This would produce a new rigorous mathematical framework for treating the effective electromagnetic transport properties for general stationary polycrystalline media, and provide a more realistic model of sea ice as a polycrystalline medium. Rigorous bounds on the effective transport coefficients, which will follow from the multicomponent composite case, will facilitate a deeper understanding of the polycrystalline nature of sea ice and the differences between columnar and granular polycrystalline microstructures, for example.

The analytic continuation method can also be adapted to provide a Stieltjes integral representation for the effective diffusivity tensor  $\kappa^*$  [1, 2], which describes the effective transport properties of a passive tracer  $T$  by a random, incompressible fluid velocity field. The propagation properties of such flows are described by the advection diffusion equation

$$\partial_t T + v \cdot \nabla T = \kappa_0 \Delta T, \quad \nabla \cdot v = 0, \quad \langle v \rangle = 0. \quad (14)$$

Here  $T(t, x, \omega)$  can be viewed as the local temperature, the positive constant  $\kappa_0$  represents the molecular diffusivity,  $v$  is a statistically homogeneous velocity field, and  $\langle \cdot \rangle$  denotes statistical averaging. Since  $v$  is incompressible, it can be represented [2] through an antisymmetric matrix  $H$ , scaled by the Péclet number  $\xi$  of the flow and  $\kappa_0$ :  $v = \kappa_0 \xi \nabla \cdot H$ . In terms of  $H$ , equation (14) can be written in divergence form as

$$\partial_t T = \nabla \cdot \kappa \nabla T, \quad \kappa = \kappa_0 (I - \xi H), \quad H + H^T = 0, \quad \langle H \rangle = 0, \quad (15)$$

where  $\kappa$  can be viewed as a local diffusivity [2]. In homogenization, we seek the long time, large distance behavior of solutions of (14). This introduces a small parameter  $\epsilon$  which can be used to obtain a

homogenized temperature [85],  $\bar{T}(x, t) = \lim_{\epsilon \downarrow 0} T(x/\epsilon, t/\epsilon^2)$ , which satisfies a diffusion equation involving the *effective diffusivity tensor*  $\kappa^*$ ,  $\bar{T}_t = \nabla \cdot \kappa^* \nabla \bar{T}$ , or in terms of  $\kappa_{jk}^* = (\kappa^*)_{jk}$

$$\frac{\partial \bar{T}}{\partial t} = \sum_{j,k} \kappa_{jk}^* \frac{\partial^2 \bar{T}}{\partial x_j \partial x_k}. \quad (16)$$

Remarkably, the effective diffusivity tensor  $\kappa^*$  is obtained in terms of a *matrix*  $E$  which satisfies equation (1) with  $J = \kappa E$  and  $\langle E \rangle = I$ , and is given by  $\kappa^* \langle E \rangle = \kappa_0 \langle E \cdot E \rangle$  [85, 2]. By the skew-symmetry of the matrix  $H$ , this formula is equivalent to equation (2) [32]. Again, due to the skew-symmetry of  $H$  the application of the spectral theorem must be slightly modified in this case [2]. The correspondence between the effective conductivity tensor  $\sigma^*$  and the effective diffusivity tensor  $\kappa^*$  is given by

$$\sigma^* = \sigma_2 \left( I - \int_0^1 \frac{d\mu(\lambda)}{s - \lambda} \right), \quad \kappa^* = \kappa_0 \left( I + \xi^2 \int_{-\infty}^{\infty} \frac{d\phi(\tau)}{1 + \xi^2 \tau^2} \right), \quad (17)$$

respectively, where  $\mu$  and  $\phi$  are matrix valued spectral measures associated with the self-adjoint operators  $\Gamma \chi_1$  and  $i\Gamma H$ . The first formula in (17) also holds for the uniaxial polycrystalline medium setting, where  $\mu$  in this case is associated with the self-adjoint operator  $\Gamma X_1$ .

Sample calculations of the spectral measure for a modified (vortical) cat's eye flow, as well as the resultant effective diffusivity as a function of the Péclet number are shown in Figure 6. We plan to investigate the spectral measures and effective transport properties of other flows relevant to sea ice motion (although it is assumed that  $\nabla \cdot v = 0$ , the current formulation serves a starting point for analysis). Attention will be paid to understanding the relations between flow geometry and spectral characteristics. Moreover, versions of the advection diffusion equation (14) serves as a model for thermal transport through sea ice in the presence of a brine velocity field, as does the Stieltjes integral for the effective thermal conductivity. We plan to use this formulation to obtain bounds and approximations for advection enhanced thermal conductivity in sea ice.

### 3.3 Composite rheology

**Analytic integral representation for the viscoelastic tensor:** Predicting the mechanical and rheological properties of the sea ice pack is important for understanding its dynamical response to winds, ocean waves, currents, and other forces. To address this problem, we plan to develop an extension of the ACM method to elastic and viscoelastic composites. Our investigations here are more mathematical in nature, focusing on the several complex variable and spectral measure aspects of the representation formulas. Their application to an ice ocean composite will require further work, although the formulation below will likely apply directly to a composite of ice floes with frazil in between, as in Fig. 2. This is a typical situation in the MIZ, and work in this direction would be important for studying ocean swell propagation in the MIZ.

Stieltjes integral representations were derived for the elements of the effective elastic stiffness tensor of a two-phase composite in [71, 72, 29, 15, 92, 103]. Further, the Stieltjes representation was extended to the viscoelastic shear modulus in torsion of a viscoelastic cylinder [143, 9], and applied to inverse homogenization [9] for successfully recovering the porosity of bone from simulated measurements of the viscoelastic shear modulus. In [22], the co-PI Cherkaev with her Ph.D. student C. Bonifasi-Lista, generalized the Stieltjes integral representation for the effective viscoelastic modulus and arbitrary loadings under the assumption that the constituents have the same elastic bulk modulus and one of the materials has a viscoelastic shear modulus while the shear modulus of the second material is elastic. The approach uses hydrostatic and deviatoric projections onto the orthogonal subspaces of the second order tensors comprised of tensors proportional to the identity tensor and trace-free tensors, given by isotropic fourth order projection tensors  $\Lambda_h$  and  $\Lambda_s$ . This enables derivation of an integral representation for the shear component of the strain  $\epsilon_s$  and for  $F(s)$ . However, the constraint is that both bulk moduli of the two materials must be equal.

This obstacle was overcome in a recent work of M. Ou [102], who developed an analytic integral representation for the case when both bulk and shear moduli of the two materials are different, extending the representation to two complex variables.

In fact, the integral representation exploiting two complex variables, was first introduced in the work of the PI Golden [44, 39] for constructing bounds for the effective properties of multi-phase random composites. For three-component media, functions of two complex variables  $m(h_1, h_2)$  and  $F(s_1, s_2) = 1 - m(h_1, h_2)$  with  $h_i = \epsilon_i/\epsilon_3$ ,  $s_i = 1/(1 - h_i)$ ,  $i = 1, 2$ , were introduced instead of  $m(h)$  and  $F(s)$  considered before. Application of Cauchy's formula for two complex variables, and special properties of the representation of

holomorphic functions with their boundary values on a polydisc, resulted in an integral representation with the measures supported on the torus  $T^2$ .

Introducing  $\zeta_j = \frac{s_j - i}{s_j + i}$ ,  $j = 1, 2$ , and  $f(\zeta_1, \zeta_2) = iF(s_1, s_2)$  with  $f(\zeta_1, \zeta_2) : D^2 \rightarrow \{Re f > 0\}$ , where  $D^2$  is a polydisc on  $\mathbb{C}^2$  plane,  $D^2 = \{|\zeta_1| < 1\} \times \{|\zeta_2| < 1\}$ , the work of the PI Golden [39] shows that  $f(\zeta_1, \zeta_2)$  is holomorphic with positive real part in  $D^2$ , and it may be represented as

$$f(\zeta_1, \zeta_2) = iImf(0, 0) + \frac{1}{2} \int_0^{2\pi} \int_0^{2\pi} (H_1 H_2 + H_1 + H_2 - 1) \mu(dt_1, dt_2), \quad (18)$$

where the kernel is a combination of functions  $H_1 = (e^{it_1} + \zeta_1)/(e^{it_1} - \zeta_1)$  and  $H_2 = (e^{it_2} + \zeta_2)/(e^{it_2} - \zeta_2)$ , and  $\mu$  is a positive Borel measure on the torus  $T^2$ . Expansion of the operator representation for  $F(s_1, s_2)$ ,

$$F(s_1, s_2) = \int P(d\omega) (s_1^{-1} \chi_1 + s_2^{-1} \chi_2) \left( (I + s_1^{-1} \Gamma \chi_1 + s_2^{-1} \Gamma \chi_2)^{-1} e_k \right) \cdot e_k,$$

into series allows (under some assumptions) characterization of the extremal measures, and construction of bounds for the effective properties of multiphase composites.

In [102], Ou was able to derive an analytic representation for the viscoelasticity problem using this integral representation formula with the measures supported on  $T^2$ . The approach is based on using projections into the hydrostatic and deviatoric subspaces with projection tensors  $\Lambda_h$  and  $\Lambda_s$  together with a clever parameterization of the bulk and shear moduli of the composite. With complex parameters  $\xi_1, \xi_2 \in \mathbb{C}^2$ , the complex bulk modulus of the composite is represented as  $\chi_1(x) \kappa_1 + \chi_2(x) (\kappa_1 + \xi_1 (\kappa_2 - \kappa_1))$ , with similar representations involving  $\xi_2$  and the shear moduli of the components  $\mu_1, \mu_2$  are used in a complex shear modulus. Here  $\kappa_1$  is the elastic and  $\kappa_2$  the viscoelastic bulk modulus of the two materials. If  $\xi_1 = 0$ , this representation gives a modulus of the elastic first material, and  $\xi_1 = 1$  corresponds to the bulk modulus in the composite. This parameterization combined with projections into the hydrostatic and deviatoric subspaces, allowed the function  $m(\xi_1, \xi_2)$  to be written as

$$m(\xi_1, \xi_2) = \frac{\bar{\epsilon}_0 : C^*(\xi_1, \xi_2) : \epsilon_0}{\bar{\epsilon}_0 : C^1 : \epsilon_0},$$

an analytic function of the complex variables  $\xi_1$  and  $\xi_2$  in  $\mathbb{C}^2$ . Here,  $C^*(\xi_1, \xi_2)$  is the effective tensor, and  $\epsilon_0$  is an averaged strain tensor. Applying the Cauchy formula and mapping to a polydisc as in [44, 39], results in a polydisc representation formula in  $\mathbb{C}^2$ . Introducing a function  $f(\zeta_1, \zeta_2) = -im(\xi_1, \xi_2)$  holomorphic in the polydisc  $D^2$  with nonnegative real part, and  $\zeta_j = \frac{1/\xi_j - i}{1/\xi_j + i}$ ,  $j = 1, 2$ , the representation (18) with the similar functions for  $H_1, H_2$ , is extended to the viscoelastic effective properties of two-phase composites.

The contrast in material properties, which in the complex permittivity case is described by a scalar, here is given by a tensor  $M = 3\xi_1(\kappa_2 - \kappa_1)\Lambda_h + 2\xi_2(\mu_2 - \mu_1)\Lambda_s$ . But as in the case of the Stieltjes representation for the complex permittivity, this polydisc integral representation for effective viscoelastic tensor separates information about the material parameters from the information about the microgeometry (though in this case, the representation depends on the elastic moduli).

**Proposed work:** We will investigate the two-parameter analytic representation of the viscoelastic effective properties of composites in  $\mathbb{C}^2$  and develop an analytic theory based on this representation. The results will be applied to the homogenization problems for sea ice in the MIZ, as discussed above.

1. We will develop an analytic theory of bounds for the effective viscoelastic properties of two-phase composites and will study extremal measures, finding the support of the convex hull of the set of measures generating the effective tensors; the images of these extremal measures under the map from measures to effective parameters, give the curves (or surfaces) bounding the set of the effective properties of the composite. These results will be applied to bounding mechanical and rheological properties.

2. We will study relationships between the geometric characteristics of the composite and the corresponding measures in the polydisc representation of the viscoelastic properties. We expect that as in the single variable case, the moments of these measures contain information about correlation functions of the microgeometry, and we will be able to use the relationships both to construct tighter bounds on mechanical properties and to extract information about the microgeometry if the effective properties are known.

3. Based on our previous experience in computing spectral measures for random transport networks [94, 97], we will develop a computational method that will allow us to numerically calculate the measures in

the analytic polydisc representation. Instead of the spaces of curl-free and divergence-free vector functions that are used in the numerical algorithms [94], we will consider projection operators to the spaces of  $\text{Ink}$ -free and  $\text{Div}$ -free tensor functions relevant in elasticity. We will digitize photographs of ice in the MIZ and use the discretized images to compute the polydisc measures.

4. We also intend to study a relationship to the spectral problem considering projections into the hydrostatic  $\Lambda_h$  and deviatoric  $\Lambda_s$  subspaces. This will provide a way to develop a more efficient numerical algorithm and will allow extension of the spectral coupling [20, 21] between the effective properties of the same composite (electromagnetic, thermal, transport, etc.) to include also mechanical properties. Such spectral coupling enables easy calculation of the properties of media using indirect measurements of different properties, or the spectral measure of  $\Gamma\chi$  computed directly from the discretized image [53].

5. Extension of the theory to  $\mathbb{C}^2$  will allow us to formulate analytic integral representations for composites with anisotropic constituents. This will be an important step in developing the analytic continuation theory that will allow application of the results to a much wider class of composites, metamaterials, polycrystalline composites, and multiphase materials. In particular, the analytic representation and numerical algorithms developed for uniaxial polycrystalline materials [61, 97] will be extended to multi-axial polycrystalline media and applied to modeling the behavior and properties of ice and ice packs.

6. Extension of the analytic continuation method to composites with anisotropic components will also allow us to develop an iterative homogenization scheme for multiscale materials. Sea ice is a multiscale material with spatial features varying on scales from mm to km. To address homogenization of such a medium, we will develop a multiscale ACM method for performing iterative homogenization on different scales. This was not possible before because of the absence of the extension of the analytic representation to anisotropic constituents, which prevented any further development. Analytic functions of several complex variables will be used to address anisotropic properties of the constituents at the finer scale; we expect that the resulting representation will be an analytic representation in the several complex variables.

The generalization of the single variable Stieltjes integral representation to a polydisc representation formula originated in previous work of the PI [44, 39] (for multi-phase composites) and was successfully extended to the elasticity problem in recent work of Ou [102]. The current proposal develops further extensions and applications of these fundamental advances. The resulting Stieltjes polydisc representation will involve a spectral measure on the torus whose moments are related to microstructural statistics. We will investigate the structure of these measures and their dependence on ice pack microgeometry and explore the application to ice pack rheology.

## 4 Broader impacts

PI Golden has developed a new upper division course, MATH 5750 / 6880 on Mathematics and Climate, and will incorporate a unit on MIZ dynamics based on this research. PI Strong has introduced a new upper division course to the University of Utah curriculum (ATMOS 5400, The Climate System), and teaches an evening session specifically for working teachers pursuing a Masters of Science in Secondary School Teaching. He will use a portion of the semester to help the teachers develop modules through which their students can explore online historical and projected sea ice variations and learn about the organisms whose habitats may be affected by projected sea ice changes.

The support and mentoring of two Ph.D. students under this project will prepare young scientists for excellence in climate research at the interface of mathematics and climate dynamics. In addition, this work will provide a rich source of data, model output, and tractable mathematical problems that can be used by the two undergraduate students to pursue research projects as part of the Math Department REU Program. This work will appeal to broad audiences through publications and presentations at research conferences focusing on sea ice, climate dynamics, and mathematical geoscience. The PI Golden, as described in the biographical sketch, has had extensive interactions with the media, and gives a large number of public lectures, providing many opportunities for outreach and making the public aware of how mathematics is being used to address the fundamental challenges of climate science.

The societal impacts of contributing to this research and inspiring and preparing future scientists to undertake further study of the polar regions are wide ranging. They are potentially global in scale since Arctic cryospheric variability exerts far reaching impacts on human accessibility to polar regions and climate dynamics through effects on atmospheric and oceanic circulations.